Progress in Electrical Engineering and Applied Physics

METAMATERIAL BASED MIMO ARRAY ANTENNA FOR MM-WAVE APPLICATIONS

Nour Elhouda Nasri[1,*], Mohammed EL GHZAOUI[2], Mohammed Fattah[1]

[1]*High School of Technology, Moulay Ismail University, Meknes*

[2]*Sidi Mohamed Ben Abdellah University, Fes, Morocco*

Abstract: This paper introduces a new 3x2 Multiple Input Multiple Output (MIMO) array antenna proposed for 28/35 GHz. Crafted with precision; it introduces a low-profile planar-patterned metamaterial (MTM) structure. It meticulously employs five interlinked ring elements to attain an efficient NZI (near-zero index) spectrum for permittivity and permeability. Highlighted in MTM unit cell are remarkable technical features, such as an expansive bandwidth of 15 GHz. Particularly noteworthy are the mu-near-zero (MNZ) and epsilon near zero (ENZ) characteristics, encompassing 15 GHz (26-41 GHz). It is worth noting that the layout employs a 2-port MIMO antenna configuration, each component intricately fashioned utilizing a 3-cell array configuration. The MTM based MIMO antenna was designed using the substrate Rogers RT/duroid 5870, highlighting a small size of 47× 45 × 0.4 mm³. The obtained outcomes shows impressive performance indicators, comprising a dual bandwidth range from 26 to 28.7 GHz and 35.15 to 35.45 GHz, isolation below −24 dB at 28 GHz and -20 dB at 35 GHz. Adding to that, the MIMO antenna exhibits excellent diversity parameters, like a mean effective gain (MEG < −3 dB), an elevated diversity gain (DG > 9.95), a low channel capacity loss (CCL < 0.4), and a diminished envelope correlation coefficient (ECC < 0.04), on both bands. The innovative MIMO antenna system utilizing MTM technology presents exceptional design and performance characteristics, rendering it appropriate for integration into 5G millimeter-wave applications.

Keywords: mm-wave, MIMO, 5G, metamaterial, dual-bandwidth, DG, ECC, MEG.

1. Introduction

Within the modern epoch, prominent advancements in 5G millimeter-wave (mm-Wave) technology and antennas have become increasingly crucial. This progress addresses the need for reduced latency cost-effective solutions, lower energy consumption, , higher data transmission speeds, and effective data transfer assistance for multiple devices across a multitude of applications outside traditional mobile communications and the cellular sector [1, 2]. Driven by limitations in available spectrum resources, current research predominantly focuses on the mm-Wave spectrum range. By utilizing MIMO technology, system channel capacity can be significantly enhanced without expanding antenna-transmitting power or using additional spectrum provisions [3]. The utilization of metamaterials in the layout of MIMO antennas for mm-wave applications has revolutionized the field by offering unique electromagnetic properties that significantly

enhance performance. Metamaterials bring significant advancements to MIMO antenna systems by manipulating electromagnetic waves in ways that traditional materials cannot. These innovative materials lead to improved performance criteria, like enhanced gain, bandwidth, and efficiency. By leveraging the unique properties of metamaterials, antenna designs can achieve better signal quality and overall system effectiveness without expanding the physical size of the antenna system. This capability is is especially beneficial in mm-wave frequencies, where space constraints and the need for compact, high-performance antennas are paramount. By incorporating metamaterials, engineers can significantly enhance antenna efficiency and system functionality, making these advanced materials essential for the future wireless communication systems development. The unique properties of metamaterials allow for better signal manipulation, resulting in improved gain, bandwidth, and overall performance.

Numerous groundbreaking antenna designs have been created and documented by researchers, spurred by the arrival of fifth-generation technology. In reference [4], for sub-6 GHz 5G applications, a MIMO antenna with four-port is designed, having gains of 4.2 dBi at 3.56 GHz and 2.8 dBi at 5.28 GHz. Reference[5] presents a dual-band MIMO antenna with quad-port designed for sub-6 GHz frequency range, achieving gains of 5.8 and 6.2 dBi at 3.3 and 3.9 GHz, respectively. Reference [6] presents a 5G millimeter-wave MIMO antenna that features a gain of around 6.6 dBi and a frequence range of 1.9 GHz (25.2-27.1 GHz) and. Introduced in reference [7], is a MIMO antenna system utilizing dielectric resonators, achieving a gain of 7 dBi and offering a bandwidth covering from 29.7 to 31.5 GHz. For 5G mm-wave applications, a dual-band MIMO antenna layout is presented in reference [8], resonating at 28 GHz and 38 GHz, achieving gains of 5.2 dBi and 5.5 dBi at these respective frequencies. Within a single negative metamaterial configuration, reference [9] describes a dual-band antenna characterized by linked square split-ring resonators. This design encompasses the frequency bands of 24-29.5 GHz and 36.7-40 GHz. A small 4-port MIMO antenna, detailed in reference [10],utilizes a defected ground structures and complementary split-ring resonators to enhance isolation. At 28 GHz, this antenna reaches an 11 dBi peak gain. Authors in [11] present a MIMO antenna with 3-ports design that incorporates metamaterials (MTM), functioning effectively in the frequency spectrum of 27.5 to 30.9 GHz. In [12], the authors designed a large band MIMO antenna that covers the frequency spectrum from 26 to 31.5 GHz. Four-port MIMO antenna in reference [13] resonating at 28 GHz is designed, and an isolation of approximately 21 dB. The authors of this article were inspired by a gap in current research on fifth-generation antenna designs to create a novel metamaterial (MTM) antenna. This new design aims to address prevalent limitations such as high mutual coupling and inadequate isolation, critical issues in covering specific 5G bands. While significant advancements have been made in this area, there remains a need for effective MTM antennas. Despite existing designs offering large bandwidths and elevated gains, overcoming these limitations is important for progressing 5G millimeter-wave communication networks.

This document unveils a novel 3 × 2 MIMO antenna design, a groundbreaking method employing metamaterials (MTM) is introduced to attain near-zero permeability and permittivity, aimed at improving the effectiveness of MIMO antenna systems. To achieve specific electromagnetic characteristics, the integration of metamaterial patches into this MIMO antenna configuration is undertaken. These characteristics like ENZ and MNZ are instrumental in advancing the design of reduced size antennas and facilitating the analysis of electromagnetic waves. It is important to highlight that the structure incorporates a 2-port MIMO antenna setup, with every element intricately developed using a 3-cell array arrangement. The MTM-based approach distinguishes itself through providing a dual-bandwidth frequency ranging from 26 to 28.8 GHz and 35.15 to 35.15 to 35.45 GHz, an isolation between MIMO radiating elements of -24 dB at 28 GHz and -20 dB at 35 GHz, a diversity gain surpassing 9.95, a small coupling coefficient (ECC) under 0.4, a mean effective gain below -3 dB, and a channel capacity loss below 0.4,. Constructed on a Rogers duroid/RT 5870 substrate, the antenna's dimensions are 47 × 45 × 0.4 mm³, and it is connected through a microstrip line with a 50 Ω match. This design is suitable for the 28/35 GHz 5G mm-Wave applications.

2. The metamaterial analysis and design and

The designed metamaterial unit cell undergoes engineering and inspection employing the HFSS (High-Frequency Structure Simulator). The MTM unit cell employs the substrate Rogers RT/duroid 5870 with a slim elevation of 0.4 mm and a dielectric constant of 2.33. Its structure comprises a compact 4 ring resonators interconnected with a square structure via a slab. Figure 1 illustrates the diagram representation of the metamaterial (MTM) unit cell engineered. The MTM cell retains a size of $W \times L = 11 \times 11\ mm^2$ with L_1=1.5 mm and W_1=9.2 mm.

To obtain the permeability and permittivity properties of the metamaterial design, a robust method is employed [14, 15], leveraging the gathered incident of scattering parameters data. At first , simulations are executed within the frequency span of 26–41 GHz to examine the S21 and S11 parameters of the designed metamaterial, as illustrated in Figure 2. The MTM spans the band from 26 to 41 GHz, encompassing the mm-wave 5G band. Utilizing the Robust Method, the metamaterial effective parameters are determined across the designated frequency spectrum. HFSS is employed for the simulation and optimization of S-parameters. Figures 3 graphically illustrate the proposed metamaterial effective parameters, encompassing both the imaginary and real constituents of the permittivity and permeability.

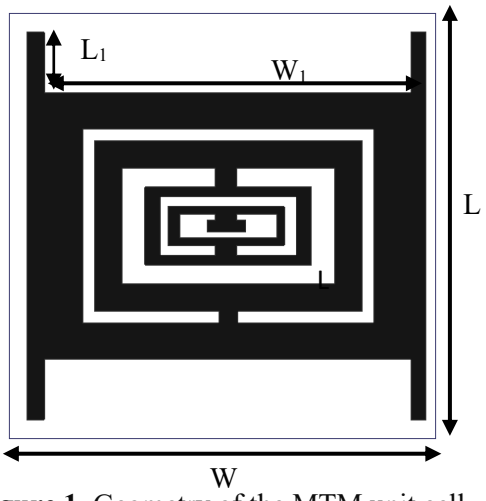

Figure 1. Geometry of the MTM unit cell.

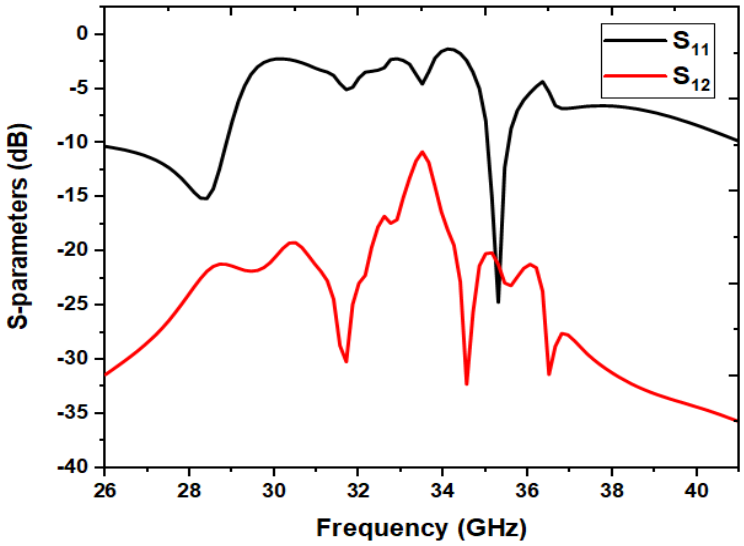

Figure 2. S-parameters of the MTM unit cell.

Across the frequency spectrum of 26 GHz to 41 GHz, Figure 3(a) illustrates the near-zero permittivity, termed "ENZ" (Epsilon Near Zero), a extremely beneficial trait in metamaterials. Moreover, Figure 3(b) depicts the permeability of the metamaterial approaching zero within the same frequency range, known as "MNZ" (Mu Near Zero). These characteristics, MNZ and ENZ, assist in the design of small antennas by enabling precise management of the electromagnetic waves, effectively reducing the antenna's physical dimensions. Furthermore, accurate convergence of electromagnetic waves are facilitated by them, leading to increased antenna gain. Tailored with innovation, the

designed metamaterial design is particularly crafted to utilize these attributes for comprehensive coverage of the 5G mm-wave band.

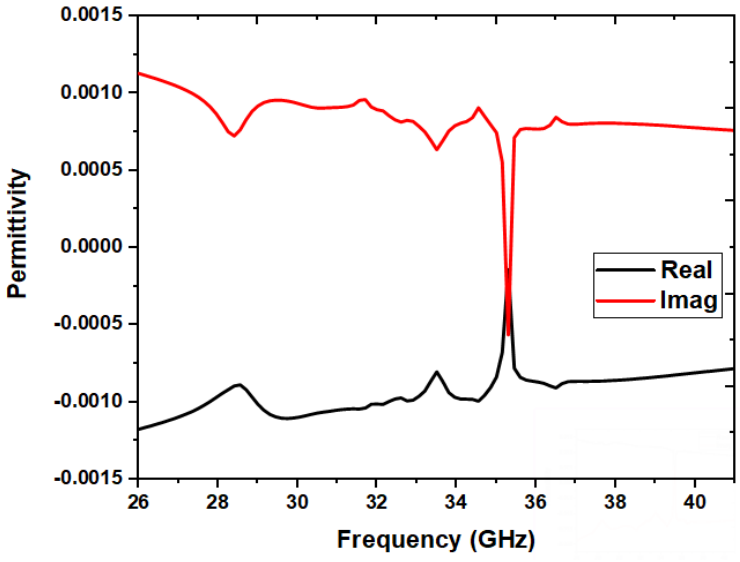

(a)

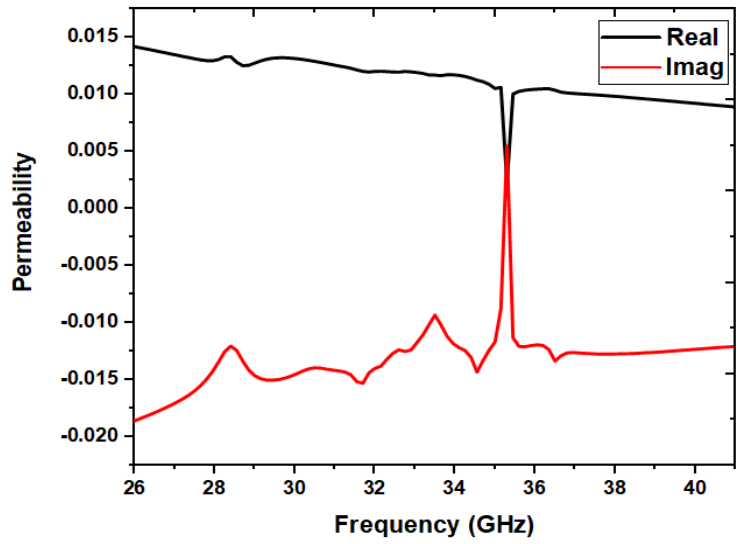

(b)

Figure 3. (a) The permittivity and (b) the permeability of the MTM unit cell.

3. Design and results of the MIMO Antenna

Utilizing metamaterials in antenna design represents an innovative method focused on improving impedance adjusment within a compact unit cell layout. As showcased in Figure 4(a), the designed MIMO antenna includes a grid of 3 × 2 MTM patches. Every grid comprises the microstrip line connecting a 3 metamaterial cells arranged horizontally. The designed MTM MIMO array antenna is illustrated in Figure 4(b). The bottom layer, in Figure 4(c), is of a rectangular shape.

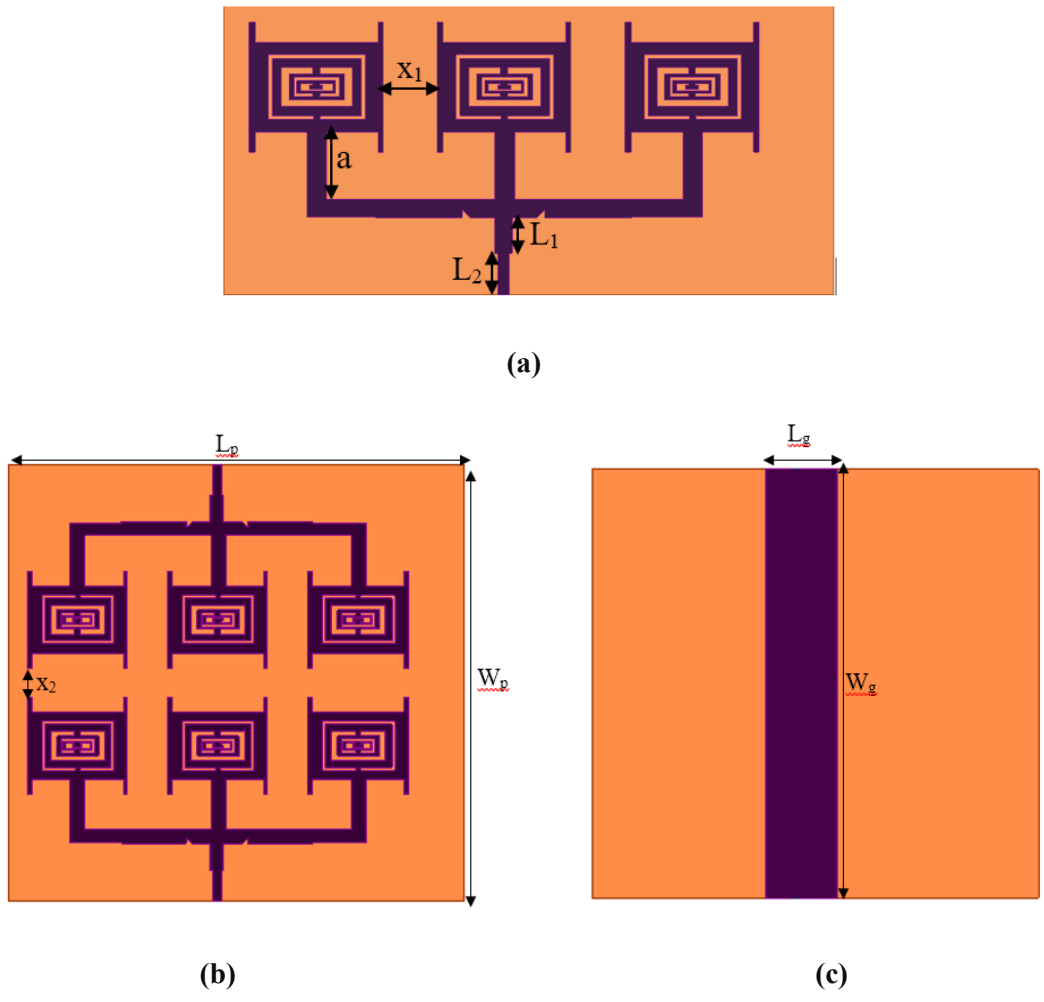

(a)

(b) **(c)**

Figure 4. The designed MTM-based MIMO antenna arrangement (a) 3-element array, (b) MIMO antenna tap layer, (c) MIMO antenna bottom layer.

The MIMO configuration features compact dimensions measuring 47 × 45× 0.4mm³. The antenna is constructed using a slim material of Rogers RT/duroid 5880, possessing a height

of 0.4 mm. Relevant antenna properties are gathered in Table 1. The engineering of the created MIMO antenna entails a dual-step procedure. Initially, a 3 × 2 MIMO antenna is created, starting with the arrangement of a setup comprising a three metamaterial units. Then the MIMO antenna was designed, covering a dual-bandwidth from 26 to 28.7 GHz (2.7 GHz) and 35.15 to 35.45 GHz (0.3 GHz), as displayed in Figure 5 (a). Regarding gain, the MIMO antenna demonstrates a value of 2.02 dBi at 28 GHz and 4.33 dBi at 35 GHz, namely superior than the array antenna gain, as presented in Figure 5(b). The shift from a one-component arrangement to a two-component MIMO antenna reveals a significant improvement in either the gain of the antenna and the impedance bandwidth characteristics.

Table 1. MTM-based MIMO antenna dimensions

Parameter	Value (mm)
x_1	4.18
a	5.21
L_1	2.24
L_2	3.2
x_2	3
L_p	47
W_p	45
L_g	7.6
W_g	45

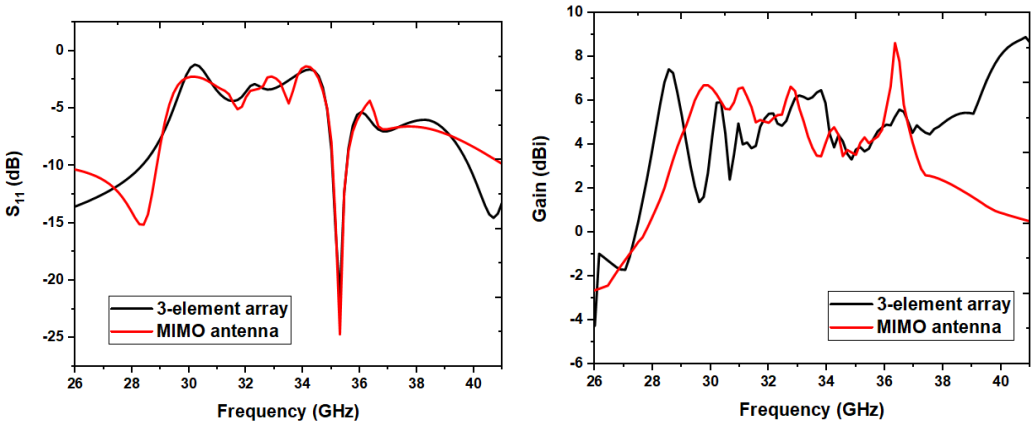

(a) (b)

Figure 5. Differences in (a) S_{11} and (b) Gain for both design steps.

4. Simulation results

The MIMO antenna in question is thoroughly simulated and analyzed utilizing HFSS (High-Frequency Structure Simulator). The evaluation of the antenna covers essential aspects like reflection coefficient, surface current distribution, radiation patterns, isolation, and gain.

4.1. S-parameters

The antenna's S_{ii}-parameters are visualized in Figure 6. The reflection coefficient, which measures the amount of power reflected back by the antenna, indicates the quality of impedance matching with the system. The designed MIMO antenna reaches a notable dual-bandwidth the first one of about 2.7 GHz (26 to 28.7 GHz) and the second one of about 0.3 GHz (35.15 to 35.45 GHz).

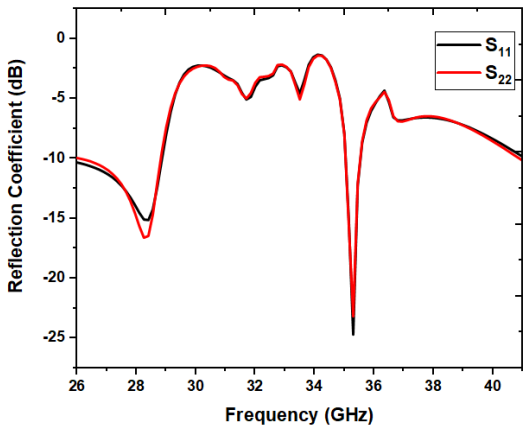

Figure 6. Reflection coefficient of the MIMO antenna.

The transmission coeffecient is a critical parameter within the context of Multiple-Input Multiple-Output (MIMO) antennas, as it quantifies the extent of coupling or interaction among each antenna elements in the array. Effective isolation guarantees that the antenna components operate autonomously, reducing interference and optimizing the overall capability of the MIMO system. Figure 7 showcases that the MIMO antenna's simulated isolation measurement is under −24 dB at 28 GHz and -20 dB at 35 GHz, indicating an adequate level of isolation. This low level of coupling means that signals received or transmitted by one component exert negligible influence on adjacent components. Minimal isolation measurement is crucial for performing MIMO system functioning, ensuring that each antenna element would be able to function autonomously without inducing notable interference among themselves.

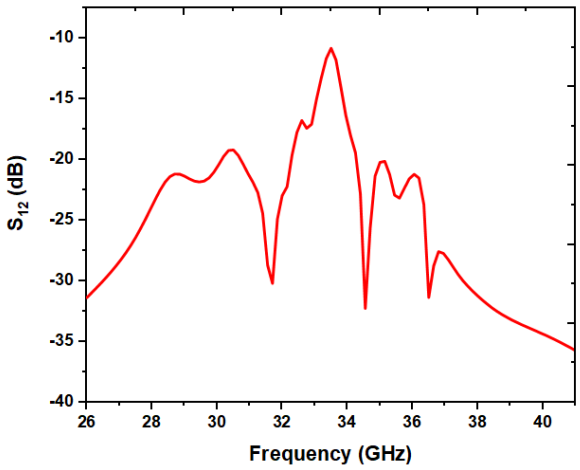

Figure 7. Isolation of the MIMO antenna.

4.2. Gain

In mm-wave wireless communication systems, the gain is vital for extending range, improving signal quality, and ensuring broad coverage. As shown in Figure 8, at 28 GHz, the MIMO antenna achieves a simulated peak gain of 2.02 dBi, and 4.33 dBi at 35 GHz.

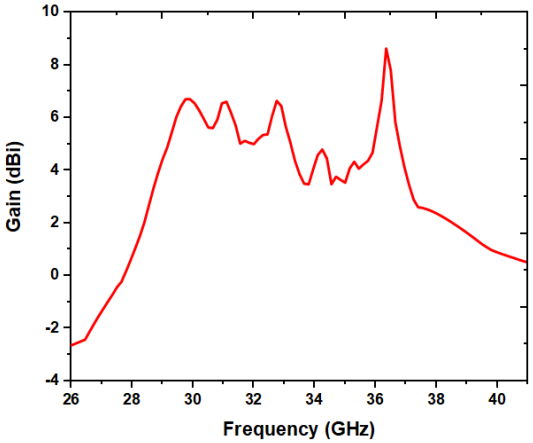

Figure 8. Gain of the MIMO antenna.

4.3. Radiation patterns

Figure 9 displays the radiation patterns H-plane and E-plane at 28 GHz and 35 GHz. At 28 GHz, as depicted in Figure 9(a), the E-plane radiation pattern and the H-plane pattern are

nearly omni-directional. At 35 GHz, E and H-planes exhibit approaching omni-directional radiation patterns, as visualized in Figure 9(b).

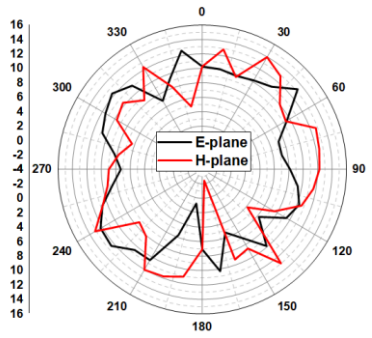

(a)

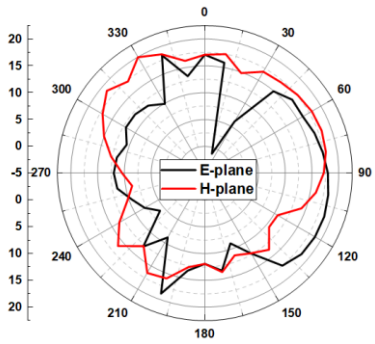

(b)

Figure 9. Radiation pattern at (a) 28 GHz and (b) 35 GHz.

4.4. Surface current distribution

In Figure 10, the distributed surface currents resulting from the simultaneous activation of both separate ports are depicted. The surface current patterns at 28 GHz and 35 GHz are examined in Figure 10(a) and (b). The principal flow of current is concentrated alongside the perimeter boundaries of the radiating elements, as illustrated in Figure 10. Additionally, the significant impact of the modified bottom layer in influencing the distribution of current is emphasized in Figure 10.

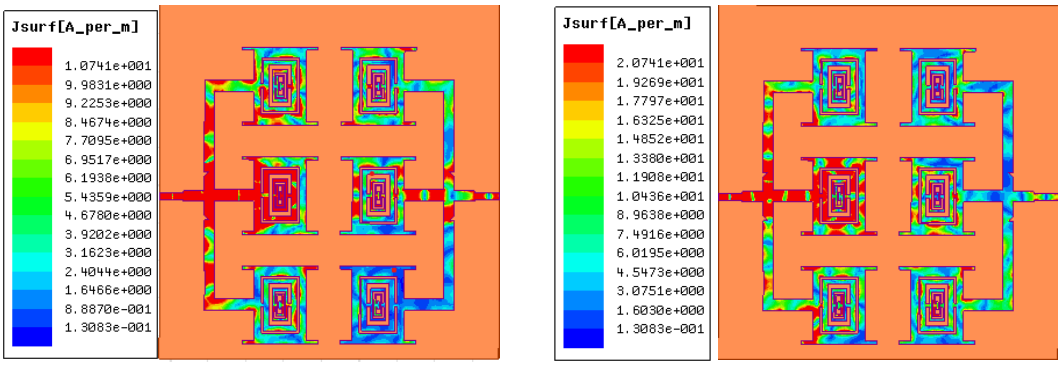

(a) (b)

Figure 10. The current distribution of the MIMO antenna at (a) 28 GHz, and (b) 35 GHz.

5. Diversity parameters

5.1. DG and ECC

In a Multiple-Input, Multiple-Output (MIMO) wireless communication system, the envelope correlation coefficient (ECC) quantifies the correlation between the envelopes of signals procured by multiple antennas, serving as a metric. It offers valuable insights into the degree of correlation in signal magnitudes received from different antennas, which can significantly influence the MIMO system performance, significantly with regards of spatial multiplexing and diversity gain. The ECC ranges amidst 0 and 1, where an elevated ECC value (near to 1) suggests robust correlation, while a minimal ECC value (near to 0) suggests minimal correlation among the antennas. Ideally, the ECC have to stay under 0.05 for optimal performance. Below is the equation for determining the envelope correlation coefficient [16]:

$$\rho_{ij} = \frac{E\{A_i(t)A_j^*(t)\}}{\sqrt{E\{A_i^2(t)\}\cdot E\{A_j^2(t)\}}} \qquad (1)$$

Where $A_i(t)$ is the envelope of the signal received at Port I, E$\{\cdot\}$ indicates the anticipated measure over time, and $A_j(t)$ is the envelope of the signal received at Port j. Figure 11 demonstrates an ECC well under 0.04 at both operating frequencies, meeting the perfect condition.

Diversity gain (DG) assesses the optimization in reliability and signal character reached by means of the utilization of several transmit or receive antennas. This metric is specifically

significant in environments prone to interference, attenuation, and unfavorable propagation circumstances. The expression for calculating diversity gain using the ECC is:

$$DG = 10\sqrt{1 - |\rho_{ij}|^2} \quad (2)$$

Within the operating band, a typical diversity gain (DG) measurement has to be above the crucial threshold of 9.95. For this MIMO antenna, the DG exceeds 9.95 at both operating bands, as illustrated in Figure 11, indicating exceptional performance.

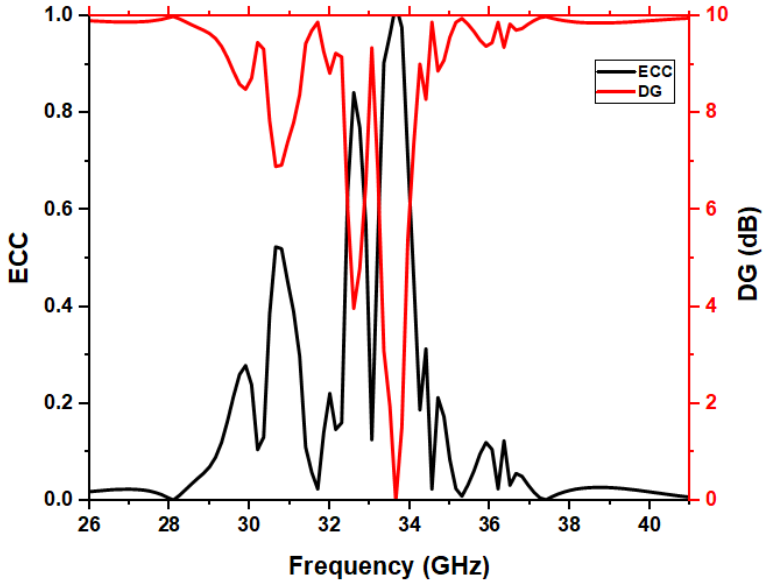

Figure 11. ECC and DG of the MIMO antenna.

5.2. CCL

Numerous physical and environmental factors compromise data integrity and diminish signal quality, leading to a cutback in the maximum realizable information transmission rate via a communication channel, known as channel capacity loss (CCL). The degradation in channel capacity is ascribed to factors such as interference, noise, inherent channel limitations, and signal degradation. These elements collectively impede the transmission of data at the theoretically maximum rate. It is crucial to keep the loss under 0.4 bits per second per hertz (bits/s/Hz) across the operational frequency spectrum. As shown in Figure 12, the CCL for our system remains under 0.3 bits/s/Hz across both resonating bands.

The calculation of channel capacity loss involves utilizing the formula [17]:

$$C_{loss} = -\log_2 \det(\alpha^R) \tag{3}$$

$$\text{Where } \alpha^R = \begin{bmatrix} \alpha_{11}\alpha_{12}\alpha_{13}\alpha_{14} \\ \alpha_{21}\alpha_{22}\alpha_{23}\alpha_{24} \\ \alpha_{31}\alpha_{32}\alpha_{33}\alpha_{34} \\ \alpha_{41}\alpha_{42}\alpha_{43}\alpha_{44} \end{bmatrix} \tag{4}$$

Where $\alpha_{ii} = 1 - \left(\sum_{j=1}^{N} |S_{ij}|^2\right)$ And $\alpha_{ij} = -(S_{ij}{}^* S_{ij} + S_{ji}{}^* S_{ij})$.

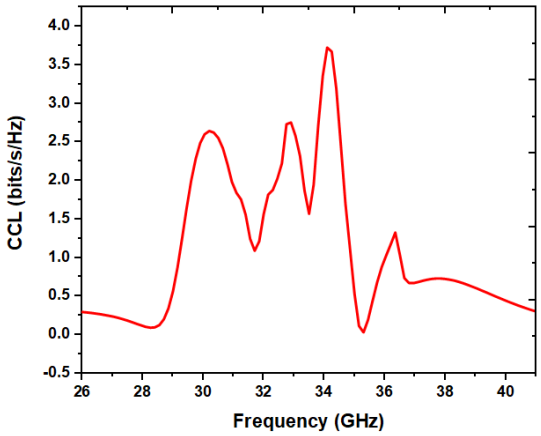

Figure 12. CCL of the MIMO antenna.

5.3. MEG

The mean effective gain (MEG) measures the mean performance or a communication system's gain, antenna, or channel under different conditions, including fading, interference, and channel variations. It offers perspectives on the usual system's performance. For optimal diversity performance, maintaining an MEG value below 3 dB is essential. As shown in Figure 13, the MEG within the operating band is kept under 3 dB. The calculation for MEG is as follows [18]:

$$MEG = \int G(\theta,\phi) * f(\theta,\phi) * d\Omega \tag{5}$$

Where $G(\theta,\phi)$ symbolizes the system's power gain at the angles θ (azimuth) and ϕ (elevation), $d\Omega$ denotes the differential solid angle element and $f(\theta,\phi)$ is the probability density function (PDF) depicting the probability of experiencing a signal situation with these particular angles.

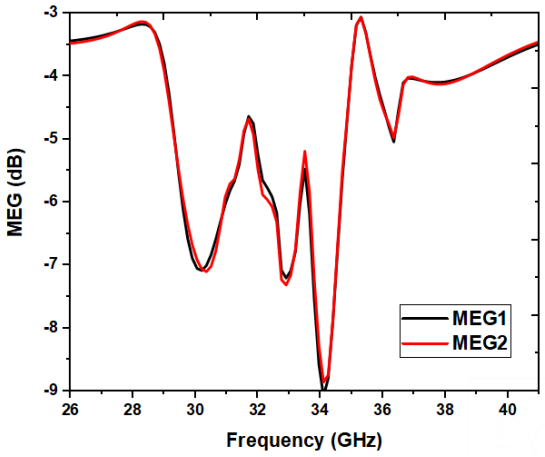

Figure 13. MEG of the MIMO antenna.

5.4. TARC

The Total Active Reflection Coefficient (TARC), which measures the extent of coupling and signal mixing between different ports. TARC provides a comprehensive assessment of how signals interact and combine within a multi-port system. This parameter is thoroughly defined in reference [16], and its calculation is based on the following expression:

$$TARC = \frac{\sqrt{\sum_{i=1}^{N}|S_{i1} + \sum_{m=2}^{N} S_{im}e^{j\theta_{m-1}}|}}{\sqrt{N}} \quad (4)$$

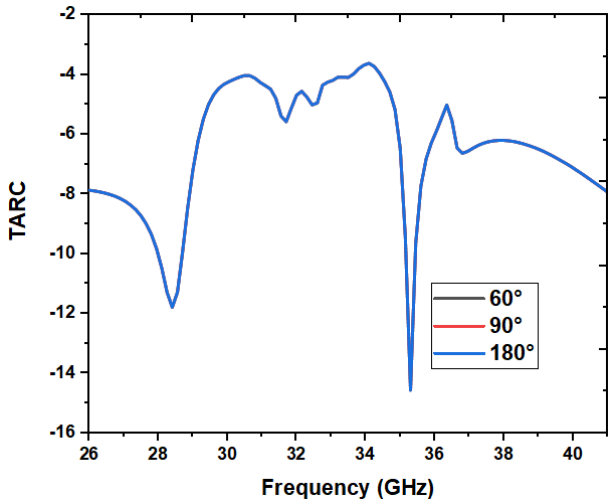

Figure 14. TARC of the MIMO antenna.

Figure 14 illustrates the simulated and calculated TARC results for various input signal phases (60°, 120°, 180°). The obtained results demonstrate that the proposed MIMO antenna array performs effectively, indicating its potential for extensive use in future 5G mm-wave applications.

6. Comparison analysis

A thorough comparative study is presented in Table 2, demonstrating the analyzed effectiveness of the antenna for 5G mm-wave applications. Despite its compact size and simple design, the findings reveal that the antenna delivers outstanding performance.

Reference	Bandwidth (GHz)	Isolation (dB)	Gain (dBi)	ECC
[4]	3.51-3.59 5.25-5.35	22 22	4.2 2.8	0.04 0.04
[5]	2.86-3.48 3.67-4.25	20 26	5.8 6.2	0.04 0.02
[6]	25.2- 27.1	30	6.60	0.002
[7]	29.7-31.5	25	7	0.02
[8]	21.4-29.35 36.6-40.4	39 38	5.2 5.5	0.0001
[9]	24.1-29.5 36.7-40	5 10	-	0.02
[10]	26.5-30.4	40	11	0.0001
[11]	27.5-30.9	40	9	-
[12]	26-31.5	25	10	-
[13]	26-31	21	10	0.0015
Proposed work	26-28.7 35.15-35.45	24 20	2.02 4.33	0.04

7. Conclusion

A cutting-edge, subtle MIMO antenna array for millimeter-wave applications has been developed using metamaterials. This innovative design includes 2 ports, each with a 1x3 arrangement of precisely designed MTM unit cells. The exploration thoroughly examines the design evolution and performance, analyzing the MTM structure, singular antennas, and the incorporated MIMO system. The results reveal the exceptional efficiency of the designed MTM design, particularly in achieving near-zero permittivity and permeability values, demonstrating its wide-ranging effectiveness. Noteworthy is the exceptional dual-bandwidth the first one of about 2.7 GHz (26 to 28.7 GHz) and the second one of about 0.3 GHz (35.15 to 35.45 GHz), an isolation level exceeding 24 dB at 28 GHz and 20 dB at 35 GHz between the MIMO antenna ports. This remarkable performance is further enhanced by the diversity criteria of the antenna, comprising DG, CCL, ECC, and MEG, exhibit

outstanding readings, guaranteeing outstanding MIMO performance throughout both operational frequency bandwidth. Additionally, the measured peak gain of about 2.02 dBi at 28 GHz and 4.33 dBi at 35 GHz, respectively, all within a compact footprint of $47\times45\times0.4$ mm^3. The developed MIMO antenna is suitable for deployment in 28/35 GHz 5G mm-wave applications.

References

[1] J. G. Andrews *et al.*, "What Will 5G Be?," *IEEE J. Sel. Areas Commun.*, vol. 32, no. 6, pp. 1065–1082, Jun. 2014, doi: 10.1109/JSAC.2014.2328098.

[2] M. L. Attiah, A. a. M. Isa, Z. Zakaria, M. K. Abdulhameed, M. K. Mohsen, and I. Ali, "A survey of mmWave user association mechanisms and spectrum sharing approaches: an overview, open issues and challenges, future research trends," *Wirel. Netw.*, vol. 26, no. 4, pp. 2487–2514, May 2020, doi: 10.1007/s11276-019-01976-x.

[3] Y. Zhang, J.-Y. Deng, M.-J. Li, D. Sun, and L.-X. Guo, "A MIMO Dielectric Resonator Antenna With Improved Isolation for 5G mm-Wave Applications," *IEEE Antennas Wirel. Propag. Lett.*, vol. 18, no. 4, pp. 747–751, Apr. 2019, doi: 10.1109/LAWP.2019.2901961.

[4] T. Upadhyaya *et al.*, "Quad-port MIMO antenna with high isolation characteristics for sub 6-GHz 5G NR communication," *Sci. Rep.*, vol. 13, no. 1, p. 19088, Nov. 2023, doi: 10.1038/s41598-023-46413-4.

[5] U. Patel and T. Upadhyaya, "Four-Port Dual-Band Multiple-Input Multiple-Output Dielectric Resonator Antenna for Sub-6 GHz 5G Communication Applications," *Micromachines*, vol. 13, no. 11, Art. no. 11, Nov. 2022, doi: 10.3390/mi13112022.

[6] Y. M. Pan, X. Qin, Y. X. Sun, and S. Y. Zheng, "A Simple Decoupling Method for 5G Millimeter-Wave MIMO Dielectric Resonator Antennas," *IEEE Trans. Antennas Propag.*, vol. 67, no. 4, pp. 2224–2234, Apr. 2019, doi: 10.1109/TAP.2019.2891456.

[7] M. S. Sharawi, S. K. Podilchak, M. T. Hussain, and Y. M. M. Antar, "Dielectric resonator based MIMO antenna system enabling millimetre-wave mobile devices," *IET Microw. Antennas Amp Propag.*, vol. 11, no. 2, pp. 287–293, Jan. 2017, doi: 10.1049/iet-map.2016.0457.

[8] B. Ali Esmail and S. Koziel, "High isolation metamaterial-based dual-band MIMO antenna for 5G millimeter-wave applications," *AEU - Int. J. Electron. Commun.*, vol. 158, p. 154470, Jan. 2023, doi: 10.1016/j.aeue.2022.154470.

[9] M. Lutful Hakim *et al.*, "Interconnected square splits ring resonator based single negative metamaterial for 5G (N258, N257, N260 and N259) band sensor/EMI shielding/and antenna applications," *Alex. Eng. J.*, vol. 81, pp. 419–436, Oct. 2023, doi: 10.1016/j.aej.2023.09.044.

[10] S. Ghosh, G. S. Baghel, and M. V. Swati, "Design of a highly-isolated, high-gain, compact 4-port MIMO antenna loaded with CSRR and DGS for millimeter wave 5G communications," *AEU - Int. J. Electron. Commun.*, vol. 169, p. 154721, Sep. 2023, doi: 10.1016/j.aeue.2023.154721.

[11] M. L. Hakim *et al.*, "Metamaterial physical property utilized antenna radiation pattern deflection for angular coverage and isolation enhancement of mm-wave 5G MIMO antenna system," *Radiat. Phys. Chem.*, vol. 209, p. 110998, Aug. 2023, doi: 10.1016/j.radphyschem.2023.110998.

[12] A. A. Ibrahim and W. A. E. Ali, "High gain, wideband and low mutual coupling AMC-based millimeter wave MIMO antenna for 5G NR networks," *AEU - Int. J. Electron. Commun.*, vol. 142, p. 153990, Dec. 2021, doi: 10.1016/j.aeue.2021.153990.

[13] Z. Wani, M. Abegaonkar, and S. Koul, "A 28-GHZ ANTENNA FOR 5G MIMO APPLICATIONS," *Prog. Electromagn. Res. Lett.*, 2018, Accessed: Jan. 22, 2024. [Online]. Available: https://www.semanticscholar.org/paper/A-28-GHZ-ANTENNA-FOR-5G-MIMO-APPLICATIONS-Wani-Abegaonkar/1f39e221eed9cf2fd6f9c5f8f77ef4775c1e5709

[14] S. S. Al-Bawri *et al.*, "Metamaterial Cell-Based Superstrate towards Bandwidth and Gain Enhancement of Quad-Band CPW-Fed Antenna for Wireless Applications," *Sensors*, vol. 20, no. 2, Art. no. 2, Jan. 2020, doi: 10.3390/s20020457.

[15] X. Chen, T. M. Grzegorczyk, B.-I. Wu, J. Pacheco, and J. A. Kong, "Robust method to retrieve the constitutive effective parameters of metamaterials," *Phys. Rev. E*, vol. 70, no. 1, p. 016608, Jul. 2004, doi: 10.1103/PhysRevE.70.016608.

[16] K. S. L. Parvathi and S. R. Gupta, "Novel dual-band EBG structure to reduce mutual coupling of air gap based MIMO antenna for 5G application," *AEU - Int. J. Electron. Commun.*, vol. 138, p. 153902, Aug. 2021, doi: 10.1016/j.aeue.2021.153902.

[17] I. Mohamed, M. Abdalla, and A. E.-A. Mitkees, "Perfect isolation performance among two-element MIMO antennas," *AEU - Int. J. Electron. Commun.*, vol. 107, pp. 21–31, Jul. 2019, doi: 10.1016/j.aeue.2019.05.014.

[18] L. M. Correia, *Wireless Flexible Personalized Communications*. USA: John Wiley & Sons, Inc., 2001.